Optimal Detection of Suspected Lung Nodules Using a Novel Convolution Neural Network

Reza Majidpourkhoei[1], Mehdi Alilou[2], Kambiz Majidzadeh[3], Amin BabazadehSangar[4]
Department of Computer engineering, Urmia Branch, Islamic Azad University, Urmia, Iran
Email: rmajidpour@yahoo.com; me.alilou@gmail.com; k.majidzadeh@iaurmia.ac.ir; bsamin2@liveutm.onmicrosoft.com

Abstract

Background and objectives: *Lung cancer is among the deadliest cancers worldwide. One of the indications of l cancers is lung nodules which can appear individually or attach to the lung wall. Therefore, the detection of so-called nodules is complicated. In such cases, the image processing algorithms are performed by the comp (CAD-x Systems), which can aid the radiologists in locating and assessing the nodule's feature. The signific problems with the current systems are the increment of the accuracy, improvement of other criteria in the res and optimization of the computation costs. The present paper's objective is to efficiently cope with aforementioned problems by a shallow and light network.*

Methods: *Convolutional Neural Networks (CNNs) were utilized to distinguish between benign or malignant l nodules. In CNN's networks, the complexity increases as the number of layers increases. Accordingly, in current paper, two scenarios are presented based on State the art and shallow CNN method in orde accurately detect lung nodules in lung CT scans. A subset of the LIDC public dataset including N=7072 slices of varying nodule sizes (1 mm to 4 mm) was also used for training and validation of the current approa*

Results: *Training and validation steps of the network were performed approximately in five hours, and the propo method achieved a high detection accuracy of 83.6% in Scenario1 and 91.7% in Scenario2. Due to the usag various validated database images and comparison with previous similar studies in terms of accuracy, proposed solution achieved a decent trade-off between criteria and saved computation costs. Thus, Scena was proposed.*

Conclusions: *The present work demonstrated that the proposed network was simple and suitable for the so-ca problems. Although the paper attempted to meet the existing challenges and fill up the prevailing niches in literature, there are still further issues that requires complementary studies to shape the tapestry of knowledge in the field.*

Keywords: *Computed Tomography, Computer Aided Detection, Deep learning, Lung nodules, Med image processing.*

1. Introduction

Low-dose CT screening in individuals with a high risk of lung cancer is proposed as an effective method of early diagnosis by various scientific communities based on the pronouncement of its potential in reducing lung cancer perishability by 20% [1]. One of the screening objectives is to detect lung nodules that are believed to be pivotal indicators in lung cancer detection from CT images. Lung nodules can be defined as round or ovoid-shaped tiny piles of tissue in the lung [2]. One of the well-known categories of lung nodule shapes is shown in figure 1. Numerous automated lung nodule detection systems have been developed to provide a second judgment and assist the radiologists in locating nodules from various CT images [2]. A sample of medical diagnostic system has been introduced in figure 2.

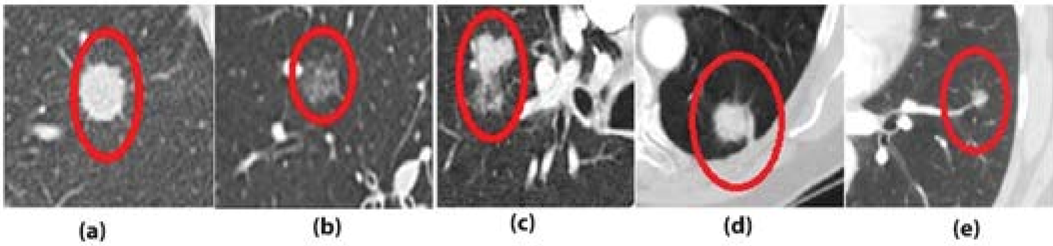

Figure 1. categories of lung nodules: (a) isolated nodule, (b) ground glass opacity(ggo) nodule, (c) mixte nodule, (d) juxta-pleural nodule and (e) juxta-vascular nodule [3]

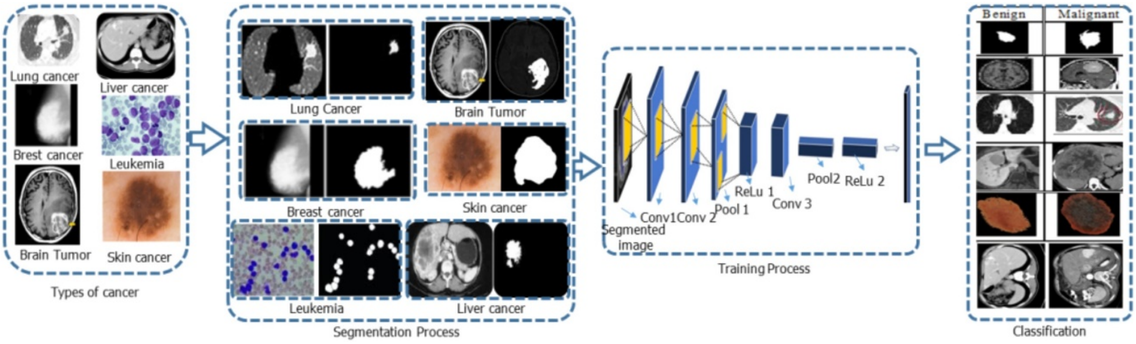

Figure 2. Machine assisted system for cancer detection in different parts of the body [4]

By and large, the automated systems include two steps: (1) the candidate screening; (2) the false-positive reduction [5]. The coarse candidates are screened by setting the threshold to the intensity and morphological parameters [6], [7]. The threshold value is commonly gentle for high sensitivity, and a large number of false-positives are generated. Hence, the advanced classifiers are required to reduce the false-positive rate. It is reported that the lung nodules with a diameter < 4 mm account for 59.5% of a total of 210 uncalcified lung nodules [8]. Besides, various recommendations have been provided for the management of micro-nodules by different institutes. For instance, the interval CT at 12 months is recommended for the subjects with a high risk once the solid nodule (< 4 mm) is detected in the baseline scan by Fleischner, Lung-RADS, and ACCP (American College of Chest Physicians) guidelines [9].

The present paper was aimed at fitting and matching the designed network with the dataset with the intention of achieving the considered purpose through heuristics. Indubitably, the heuristics with the accepted results were compared for a second round with the results of previous studies. It is believed that the implementation of state-of-the-art CAD was essential to support radiologists' decisions. Thus, with a better CNN design, more eminent results could be achieved with fewer crops and epochs[10]. Therefore, the number of CNN layers or, in other words, the CNN models with different depths in the current paper was examined.

2. Literature Review

Deep learning is an artificial intelligence subspecialty that focuses on imitating human abstraction capabilities by dynamically changing its neural network functions parameter to do extra accurate detection and classification. The abstraction capability of deep learning, especially Convolutional Neural Network(CNN) as the current state-of-the-art approach for image analysis, was recently examined in medical images In the past decade [11-14].

Succinctly, convolutional neural networks consist of a disparate layers stack, which is accordingly learned to automatically extract useful information from the input data without involving any features of engineering procedures [15]. A typical CNN architecture is illustrated in figure 3.

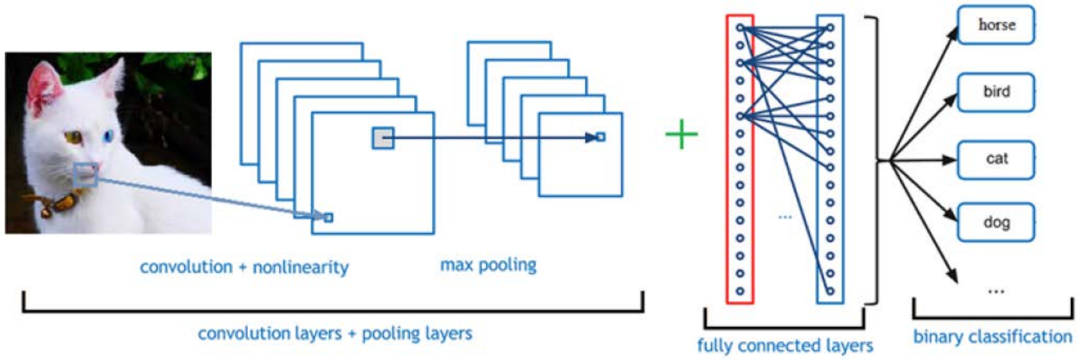

Figure 3. A typical CNN architecture [16]

The first CNN was the LeNet, presented in the 1998 paper[17]. This was the first network in which convolution filters were used[17,18]. Later on, a number of much deeper CNN structures were suggested[17] comprising AlexNet that was designed by Alex Kryshevsky, contained eight layers, was the basis of the convolutional neural networks applied to the ILSVRC-2012 challenge[19], first successful application of CNN in a recognition task, and VGG-VD with 16 and 19 layers of CNN structures. GoogleNet had a 22 layer network that contains basic architectures and was proposed to control the confutation between increasing the training parameters and overfitting[20]. Residual Network(ResNet) was approximately 20 times deeper than AlexNet and eight times deeper than VGGNet[21]. Furthermore, SENet[22] and their variants [21], [23].

Most of the previously mentioned algorithms utilized complicated, exceedingly deep, or pre-trained CNNs that are not built specifically for the lung nodule classification problem. Thus, they require extra computations and far more running times to reach substantial hours on advanced hardware to achieve a final outcome. Our contribution can be summarized as follows:

- ✓ Selection of simple network architectures and discovering the best configuration by experiments yielded to an optimal lightweight network that avoids overfitting and performs well
- ✓ Benefiting from a novel end-to-end and supervised learning manner and customized patch-based CNN for the image classification, which reduces the computational costs and training time of the whole framework

- ✓ Sufficient, valid, and realistic samples for training
- ✓ The number of suitable cycles of the learning phase for agility
- ✓ Performance improvements from the low number of CNN layers
- ✓ Meliorate evaluation criteria, such as accuracy, sensitivity, and specificity, as well as reducing the false-positive rate and computational time, which are the main challenges of the previous studies

3. MATERIALS AND METHODS

3.1 Dataset

One of the challenges in implementing deep learning algorithms is the lack of appropriately labeled medical image data. The so-called limitation, which pertains to most of the deep learning applications, is primarily due to patient's medical information confidentiality. One of the publicly available lung CT image datasets is LIDC/IDRI database[24]. Since the entirety of the LIDC dataset has a massive size (125 Gigabytes), a subset of the dataset, including a number of 3536 positive and 3536 negative samples/slices, was extracted from 300 CT scans and used in the present experiment. Positive samples corresponded to a set of 2D image regions/patches with the size of 80*80 pixels and a nodule manifestation. In contrast, the negative samples corresponded to the same size patches inside lung parenchyma without a nodule. Accordingly, a subset of the LIDC public dataset, including N=7072 CT slices of varying nodule sizes (1 mm to 4 mm), was used for the training and validation of the proposed approach.

3.2 Policies to distinguish between small lung nodules and non-nodules from CT images

Generally, there were three policies to distinguish between lung micro-nodules (or small nodules) and non-nodules from CT images. First, the CNN models were utilized to refrain from a series of computationally exorbitant steps such as segmentation, feature extraction, and selection that lead to the end-to-end solution. Likewise, the residual CNN was employed to reduce the false-positives [25], the massive-training artificial neural networks (MTANNs) were also used to build up the end-to-end machine-learning models given the bounded training data [26]. To address the issue of data lack, data augmentation and transfer learning were proposed [12]. Although data augmentation (i.e., rotation, translation, and scale) are typically attempted to be exploited in studies, no considerable improvements were found for performance measures (i.e., the F-score, accuracy, sensitivity, and AUC)[27]. Second, the hand-crafted features-based classifiers were widely applied. Based on border delineation or segmentation, various features have been considered, including intensity, morphology, texture, wavelets, etc.[28], [29], [30]. Subsequently, the feature selection and machine learning-based methods were followed [31], [32]. For instance, to characterize the lung cancer phenotypes, Parmar et al. [33] evaluated 14 feature selection algorithms with 12 classification methods and found that the Wilcoxon test-based feature selection method, as well as random forest, achieved the highest performance. Third, the fusion of CNN estimation and hand-crafted features was also used to address the false-positive reduction in the automated detection of nodules [2]. Even though it is difficult to decide on the best strategy to be applied, the proposed CNN models presented a solution with appropriate performance to classify micro-nodules and non-nodules.

3.3 Proposed model

A usual framework of nodule detection is shown in Figure 4. The workflow of the proposed framework is revealed in Figure 5. The framework included the steps of Pre-Processing, Segmentation, Automatic Identification (extraction of features regardless of specific features and based on the convolutional network, and then network training using dataset), and Classification based on the CNN algorithm (and Non-traditional). According to the objectives of the research (especially noted in section 2). Above all, Fast analysis, high accuracy, low False-Positive Rate, and a primary light model implemented on our dataset, and to improve these results, innovative changes were applied to this CNN model, with its effects being observed several times. Finally, the optimized architecture was achieved that was compatible with the present dataset and the current study's objectives. The proposed CNN architecture was a modified version of the proposed architecture in [26]. The main difference between the two architectures was the number of their layers.

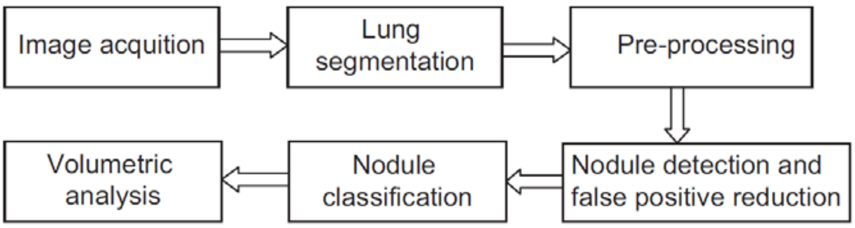

Figure 4. Usual framework of nodule detection and analysis systems [34]

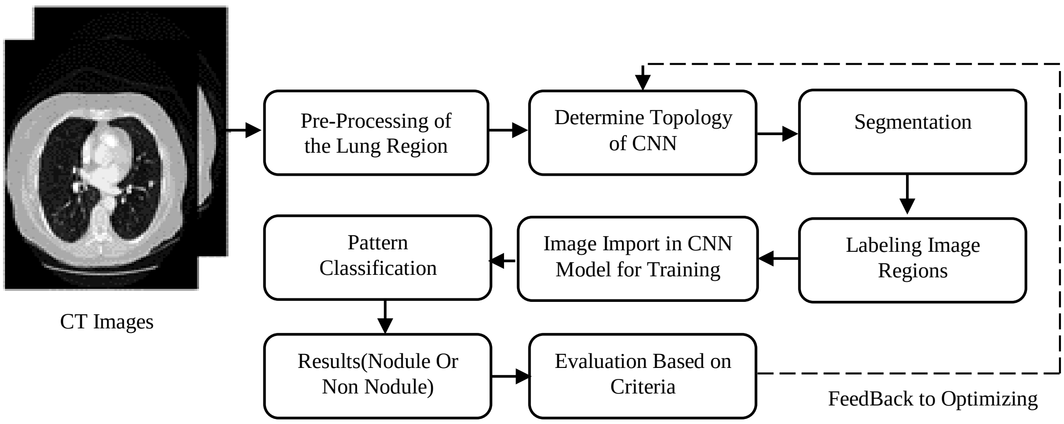

Figure 5. The proposed framework and model

Large images' input may take a longer time and result in impoverished feature learning (especially for tiny objects). The numerous existing deep learning-based methods' computation capacity were conditioned through the available memory on the Graphics Processing Units (GPUs), making it nearly impossible to apply deep CNN-based methods for processing extra-large images [35]. Consequently, to remedy the memory requirement, it was necessary to split the large images into small patches comprising the objects whose features needed to be detected. In addition, large image patches might contain a substantial amount of unnecessary information, which could cause a mixed-pixel problem [36]. In the segmentation step, classifying at the pixel level, extracting the lung's main areas from the background, and removing additional parts as well as adjacent tissues from the image were the intentions of the present research. Considering that the results of this stage were used in the following steps of the same convolutional model, and the convolution model requires capacious memory to execute, the importance and necessity of segmentation were well known. To perform segmentation operations, traditional image processing algorithms, such as the Water-Shield, Active Connector, etc., and even the CNN model, could be employed using MatLab software. In Figure 6, the output of the lung segmentation is exhibited.

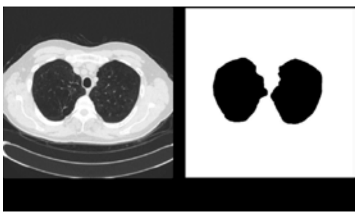

Figure 6. Output of lung segmentation: (left) the original image and (right) the segmented image

The second step was to determine the training strategy and data preparation, including pre-processing and multi-partitioning of images and positive/negative tagging samples. In fact, the step led to data preparation, due to which a CT scan of a patient consisted of n numbers. For example, in 200 slices, each slice was a cut of tissue (although some slices were removed in the first step), and each slice was a two-dimensional image with the size of 512 * 512 mm. Therefore, the digital information of a patient's CT scan image was initially stored in a 3-D array. In the received data, a file called Coordinative meant a two-dimensional coordinate guide that expressed the coordinates of the probability and extended the presence of the nodule. The operation began on the 3rd array above, and the two-dimensional slices were converted to smaller sections, such as 80×80mm. The coordinates of each of these sections were analogous to the coordinative file, and once the result was positive, it was stored as a Box or a Separation Crop (Figures 7,8) with a positive label. Otherwise, it was labeled as Negative.

Figure 7. Cropping of Slice

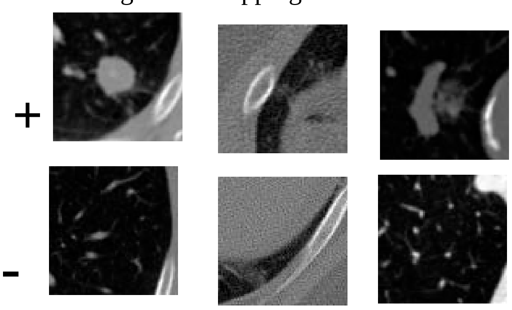

Figure 8. Labeling Data Images

The information for each of these sections, including the primary coordinates, digital information, and the image itself, ought to be stored for later stages. The above items were stored for the entire patient, and the results were collected as a tagged data. Although the CNN could potentially be trained in all pixels, an increase in computational costs and training time lead the researcher to cut the images around the coordinates provided in the annotation file (Coordinate file).

Latterly, the number of deep CNNs layers became larger and larger. It was beneficial to increase the number of layers in the network since the features could be quickly learned at different abstraction levels. Using very deep network structures requires extra parameters to be recognized, leading to an increase in the network complexity, the training time, the error generalization, and the overfitting rate.

Various research was done regarding the lung nodule detection and state-of-the-art CNN method, which is noted in section 2. In the present inquiry, an agile CNN model was developed, which included two and three convolutional layers, where the most successful model was not the deepest one but the one with two convolutional layers. Hence, the deeper CNN structures were not reasonable all along, and it was crucial to take the following factors into consideration while designing a network: the size and shape of the objects to be classified, the available dataset, and a number of parameters, such as kernels size that were not merely relied on the network depth, The study conducted by Tajbakhsh et al. [26] are shown in figure 9. Besides, the study conducted by El-Regaily et al. [37] is shown in figure 10.

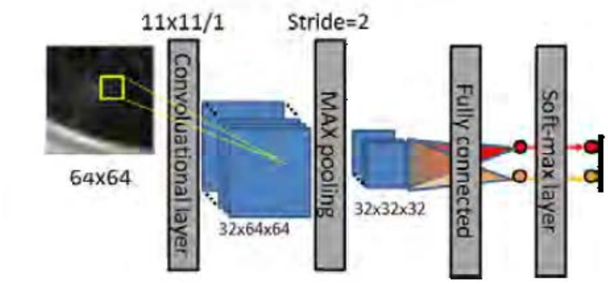

Figure 9. A shallow CNN(sh-CNN) [26]

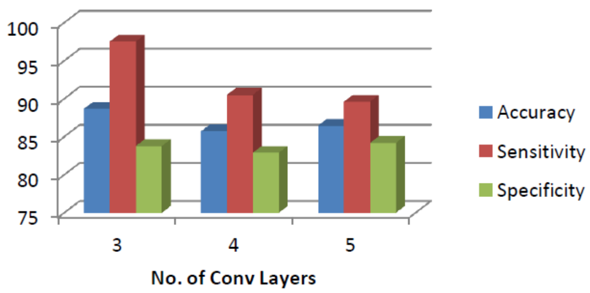

Figure 10. The effect of changing the number of convolutional layers on the average accuracy, sensitivity and specificity [37]

The third step, the CNN model, was the main stage and was designed using the following equations: the convolutional layer is shown in equation (1) [38].

$$f^j = PReLU(\sum_i c^{ij} * f^i + b^j) \quad (1)$$

f^i: i-th input attribute to be mapped
f^j: j-th Output feature that is mapped
b^j: bias for the j-th output attribute that is mapped
c^{ij}: Kernel and convolutional core among f^i and f^j

After each layer Conv. A PReLU unit(Parametric Rectified Lineral Unit) converts nonlinear mode linearly, according to equation (2) [39].

$$PReLU(f^j) = \begin{Bmatrix} f^j & if & f^j > 0 \\ a_j f^j & if & f^j \leq 0 \end{Bmatrix} \quad (2)$$

a_j : The learning parameter, for example, 0.25

Pooling layer or parameter reduction is shown equation (3) [19].

$$C_{pooled} = \begin{bmatrix} pool(\propto (c_1 + b_1 * e))) \\ . \\ . \\ pool(\propto (c_n + b_n * e)) \end{bmatrix} \quad (3)$$

$\propto ()$: Activation function as Max or Average
c_i : i-th Convolution property vector
b: The bias of each feature vector
e: Vector unit, same size with c_i

Two state Soft-Max function is placed in the last layer and used to obtain the probability functions for each positive or negative label, and the main purpose is to increase the probability and reduce entropy, that shown equation (4).

$$P_k = \frac{\text{EXP}(O_k)}{\sum_{h\subseteq\{0,1\}} \text{EXP}(O_h)} \quad (4)$$

P_k : Likelihood of each tag
O_k : k-th Output

Zero means negative label and one means positive label. The Loss function is used to reduce the entropy during the training, according to equation (5) [40].

$$L(w) = -\frac{1}{N}\sum_{n=1}^{N}[y_n \, Log \;\hat{y}_n + (1-y_n)Log(1-\hat{y}_n)] + \lambda|w| \quad (5)$$

N: Training sample number
$\hat{y}_n$: Predictable Chance for CNN
$\lambda|w|$=5*10^{-4}

Weights are plotted by the SGD algorithm during training, according to equation (6) [41].

$$w_{t+1} = w_t + v_{t+1} \qquad v_{t+1} = \mu \, v_t - \propto \nabla L(w_t) \quad (6)$$

t: Repeat Sample Number
v: updated value, whose initial value is zero
α : Training rate
The initial training rate is: $\propto_0 = 6 * 10^{-5}$
μ=0.9
$\nabla L(w)$: gradient proportionaled to size of the data

Calculate the training rate according to equation (7) [42].

$$\propto_{t+1} = \propto_0 (1+\gamma t)^{-p} \quad (7)$$

$\gamma = 0.0001$ p=0.75

Considering the fact that the micro-nodules and non-nodules were both tiny objects, two CNN models were designed with small filters and different depths. The first CNN model (Scenario1) consisted of three convolutional layers (according to Figure 11 and Table 1), and the second CNN model (Scenario2) consisted of two convolutional layers (according to Figure 12 and Table 2). The dropout layer helped the network to ignore a series of units during the training process, which could overcome the overfitting problem. The ReLU layer played the role of convergence accelerator of the stochastic gradient descent (SGD), resulting in the recovery of the training speed. MaxPooling layer facilitated the network to focus merely on the image information deriving from the convolution process [43].

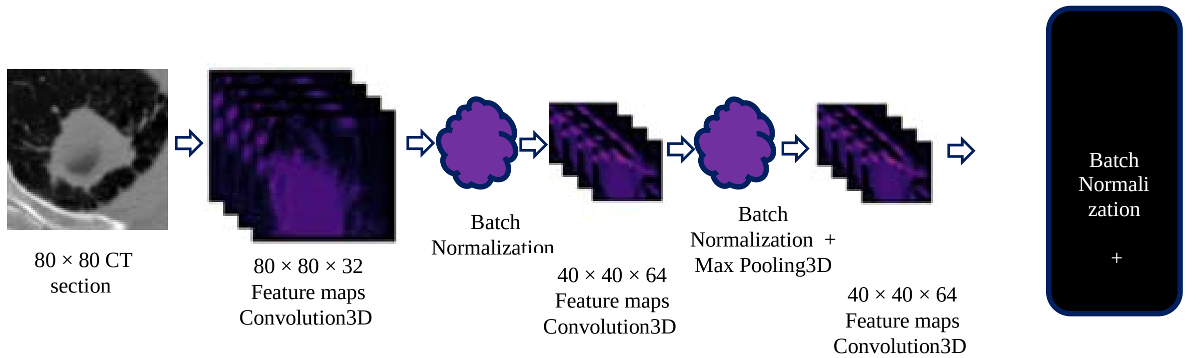

Figure 11. Proposed CNN architecture of Scenario1

Table 1. Parameters of the CNN architecture of Scenario1(Dropout=0.2 and Learning Rate=0.0001)

Layer (type)	Output Shape	Param #
conv3d_4 (Conv3D)	(None, 39, 39, 3, 8)	80
batch_normalization_4 (Batch	(None, 39, 39, 3, 8)	32
conv3d_5 (Conv3D)	(None, 19, 19, 3, 8)	584
batch_normalization_5 (Batch	(None, 19, 19, 3, 8)	32
max_pooling3d_2 (MaxPooling3	(None, 9, 9, 3, 8)	0
conv3d_6 (Conv3D)	(None, 4, 4, 3, 8)	584
batch_normalization_6 (Batch	(None, 4, 4, 3, 8)	32

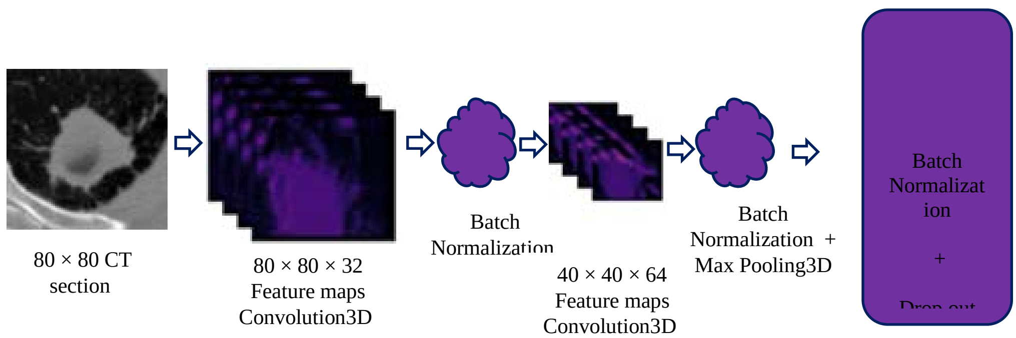

Figure 12. Proposed CNN architecture of Scenario2

Table 2. Parameters of the CNN architecture of Scenario2(Dropout=0.2 and Learning Rate=0.0001)

Layer (type)	Output Shape	Param #
conv3d_3 (Conv3D)	(None, 39, 39, 3, 8)	80
batch_normalization_3 (Batch	(None, 39, 39, 3, 8)	32
conv3d_4 (Conv3D)	(None, 19, 19, 3, 8)	584
batch_normalization_4 (Batch	(None, 19, 19, 3, 8)	32
max_pooling3d_2 (MaxPooling3	(None, 9, 9, 3, 8)	0

The tagged data from the previous step was divided into three groups: training, validating, and testing. The data was imported into a model based on a simplified standard Le-Net model and carried out training, validation, and testing steps. Indeed, the steps were taken to extract the features, categorize the features, and correct the weights. The final and extra accurate diagnosis (the nodule coordinates in the box) was automatically carried out by the CNN model. Thenceforth, all the model evaluation criteria (including the Confusion matrix and various types of plots, such as CNN graphical shape and evaluation charts) were extracted. Quality assessment parameters such as Accuracy, False-Positive, etc., were calculated. Once the criteria did not obtain the desired utility of previous research, changes in the layers, as well as the number and arrangements of the model, were made ad-hoc, and the steps were repeated. The proposed CNN architecture with 400 iterations(epochs) was exploited.

A hardware configuration was benefited for implementing the existing research, including a Core i5 2.4GHz Processor, 8GB of RAM, and Intel Graphics 520. Matlab software was also used to prepare and pre-process images, import data, and isolate the lung from the background. Python was the primary programming language selected for project development. Anaconda3 (64-bit), Jupyter Notebook, Tensorflow, and Keras libraries were utilized to implement the CNN network. Keras was compatible with Python 2.7, 3.6. Correspondingly, Keras allowed users to use other Python libraries, including SciPy, NumPy, matplotlib, sklearn, and Tflearn.

4. RESULTS

The main variables or criteria for evaluating the proposed algorithm's efficiency were loss function, and Classification Accuracy (e.i., how much recognition is close to reality) were obtained by dividing the number of samples which were categorized into the total number of samples and Loss Function[44]. In the present study, the 5-Cross Validation Method was used for the learning and testing steps. Thus, after training the CNN model, the model was tested with 1415 images, and the average time to run the system was five hours. The Loss and Accuracy Plots of two Scenarios shown in Figures 13,14,15,16:

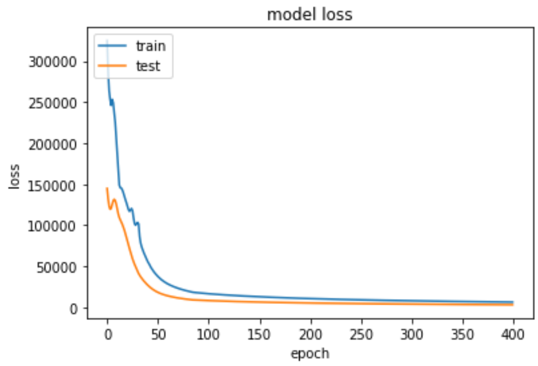

Figure 13. The Loss Curve of Scenario1

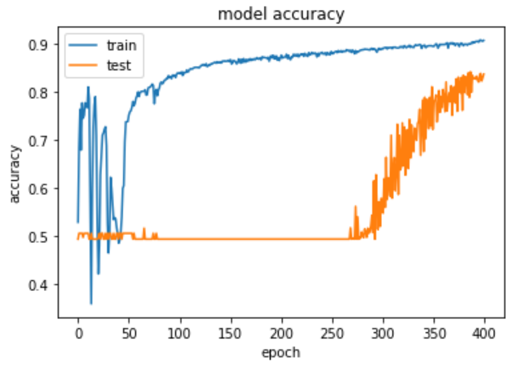

Figure 14. The Accuracy Curve of Scenario1

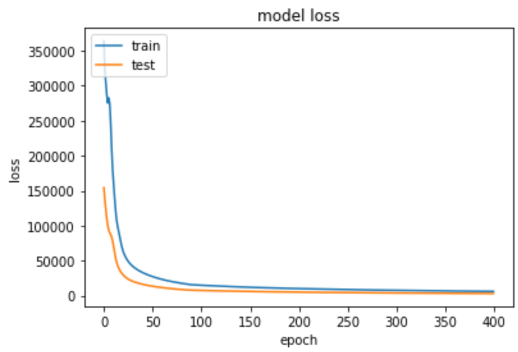

Figure 15. The Loss Curve of Scenario2

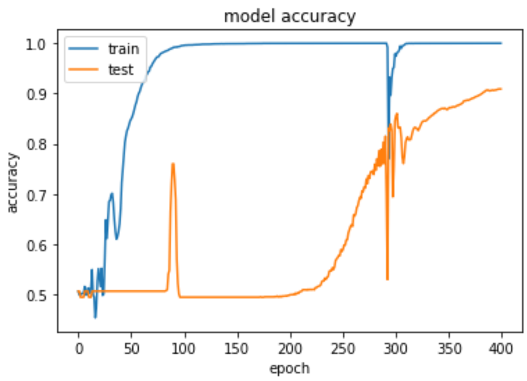

Figure 16. The Accuracy Curve of Scenario2

The proposed CNN models with suitable depth and size of image patches could effectively and efficiently differentiate between lung micro-nodules (diameter < 4 mm) and non-nodules and reduced the false-positive rate. Small image patches (or the receptive field) might lead to significant performance for the tiny objects. The deeper CNN structures were not always nice, and it was pivotal to consider the dataset and the objects of interest while finding adequate depth. Some parameters such as kernel size and the number of epochs required to be optimized. These methodological findings and the extracted dataset of micro-nodules and non-nodules might help to design other CNN models. The proposed CNN models might help to decrease the radiologists' workload, unnecessary anxiety for the affected subjects, contribute to precise lung cancer management in early stages, and automatic lung nodules detection from CT images.

Table 3 presented a comparison between the current approach and other similar published methods. According to this comparison and the plethora of similar studies with comparable findings that have been mentioned in the literature, it can be seen that the evaluation criteria were improved in a balanced state. Therefore the proposed method provided an acceptable performance.

Table 3 Comparison of the proposed method with previous similar studies

Nodule Detection Method	Database	Number of Used CT Images	Sensitivity %	Specificity %	Accuracy %
Multi-scale Convolutional Neural Networks (MCNN)[45]	LIDC-IDRI	1010	NA	NA	86.84
Multi crop convolution neural network[46]	LIDC-IDRI	1010	77	93	87.14
CNN[47]	LIDC-IDRI	4581	83.96	84.32	84.15
CNN 5 Layer[48]	LIDC-IDRI	1000	78.19	86.13	82.1
ReCTnet[49]	LIDC-IDRI	1018	90.5	NA	NA
CNN U-NET[50]	LUNA16	1397	NA	NA	86.6
2D ConvNets[7]	LIDC-IDRI	888	85.4 and 90.1	NA	NA
Attention 3D-CNN[51]	Lung Nodule Analysis 2016 (LUNA16)	888	95.8	NA	NA
2D convolutional neural network (CNN) & (Faster R-CNN)[52]	LUNA16	1018	86.42, 73.4 and 74.4	NA	NA
Level-Set Method[53]	LIDC-IRDI	800	84.3	85.9	84.8
Pixon Based Method[54]	LIDC-IRDI	800	78.8	81.2	80.4
	ELCAP	50	72.5	60	67.5
Proposed Method	Scenario1 LIDC-IRDI	300 CTs 7072 patches	NA	NA	83.6
	Scenario2 LIDC-IRDI	300 CTs 7072 patches	NA	NA	91.7

5. CONCLUSION AND FUTURE WORK

Correct lung disease diagnosis with no delays following the onset and proper treatment of the illness is of extra necessity and cruciality. Diagnosis of lung diseases requires a careful and time-consuming process that is undertaken by a specialist physician. Obviously, human error due to the large number and complexity of images is effective in diagnosing and treatment process. Given the increasing spread of lung diseases in nowadays' industrialized societies, the provision of computerized methods to aid faster and precise diagnosis is among physicians and engineers' main concerns. Thus, with the intention of reducing human errors, speeding up diagnosis, and increasing their accuracy and precision, a CAD system for assisting the physicians was presented in the current paper.

A simple yet efficient CNN architecture was developed that suited nodule detection. Using a CNN greatly simplified the training process and shortened the training time without sacrificing the classification accuracy, which outperformed several state-of-the-art algorithms and was comparable to the others.

two CNN models were developed to differentiate micro-nodules and non-nodules from CT images. These models could optimize the accuracy in automated lung nodule detection, which consequently reduced the radiologists' workload, avoided unnecessary anxiety for the affected subjects, and helped imply extra accurate follow-ups leading to proper and life-saving treatments. The proposed method had the desired efficiency and speed of detection. By comparing the diagrams results of the two scenarios, it was unearthed that Scenario 2 was more efficient owing to its lightweight network.

It could be a question of future research to investigate the relationship between the other independent variables and the evaluation parameters. Furthermore, a Mobile app could be developed based on the proposed model for public uses. In addition, in the present study, merely the dataset of LIDC was exploited, and the generalizability of our CNN model was not known for other independent datasets. Therefore, this could be a decent research question for future studies to explore with the intention of extending the current model's capacity to determine the nodules as well as tagging them as cancerous or not.

Acknowledgements The authors thank the potential reviewer's for their constructive comments and suggestions that greatly contributed to improving this article.

Compliance with ethical standards

Conflict of interest Authors, Reza Majidpourkhoei, Mehdi Alilou, Kambiz Majidzadeh and Amin BabazadehSangar, declare that they have no conflict of interest.

Ethical approval This article does not contain any studies with human participants or animals performed by any of the authors.

REFERENCES

[1] National Lung Screening Trial Research Team. (2011). Reduced lung-cancer mortality with low-dose computed tomographic screening. New England Journal of Medicine, 365(5), 395-409.

[2] Teramoto, A., Fujita, H., Yamamuro, O., & Tamaki, T. (2016). Automated detection of pulmonary nodules in PET/CT images: Ensemble false-positive reduction using a convolutional neural network technique. Medical physics, 43(6Part1), 2821-2827.

[3] Mastouri, R., Khlifa, N., Neji, H., & Hantous-Zannad, S. (2020). Deep learning-based CAD schemes for the detection and classification of lung nodules from CT images: A survey. Journal of X-Ray Science and Technology, (Preprint), 1-27.

[4] Saba, T. (2020). Recent advancement in cancer detection using machine learning: Systematic survey of decades, comparisons and challenges. Journal of Infection and Public Health, 13(9), 1274-1289.

[5] Dou, Q., Chen, H., Yu, L., Qin, J., & Heng, P. A. (2016). Multilevel contextual 3-D CNNs for false positive reduction in pulmonary nodule detection. IEEE Transactions on Biomedical Engineering, 64(7), 1558-1567.

[6] Jacobs, C., van Rikxoort, E. M., Twellmann, T., Scholten, E. T., de Jong, P. A., Kuhnigk, J. M., ... & van Ginneken, B. (2014). Automatic detection of subsolid pulmonary nodules in thoracic computed tomography images. Medical image analysis, 18(2), 374-384.

[7] Setio, A. A. A., Ciompi, F., Litjens, G., Gerke, P., Jacobs, C., Van Riel, S. J., ... & van Ginneken, B. (2016). Pulmonary nodule detection in CT images: false positive reduction using multi-view convolutional networks. IEEE transactions on medical imaging, 35(5), 1160-1169.

[8] Azharuddin, M., Adamo, N., Malik, A., & Livornese, D. S. (2018). Evaluating pulmonary nodules to detect lung cancer: Does Fleischner criteria really work?. Journal of Cancer Research and Practice, 5(1), 13-19.

[9] Ruparel, M., Quaife, S. L., Navani, N., Wardle, J., Janes, S. M., & Baldwin, D. R. (2016). Pulmonary nodules and CT screening: the past, present and future. Thorax, 71(4), 367-375.

[10] Liu, S., & Deng, W. (2015, November). Very deep convolutional neural network based image classification using small training sample size. In 2015 3rd IAPR Asian conference on pattern recognition (ACPR) (pp. 730-734). IEEE.

[11] Hua, K. L., Hsu, C. H., Hidayati, S. C., Cheng, W. H., & Chen, Y. J. (2015). Computer-aided classification of lung nodules on computed tomography images via deep learning technique. OncoTargets and therapy, 8, 2015–2022.

[12] Greenspan, H., Van Ginneken, B., & Summers, R. M. (2016). Guest editorial deep learning in medical imaging: Overview and future promise of an exciting new technique. IEEE Transactions on Medical Imaging, 35(5), 1153-1159.

[13] Ongsulee, P. (2017, November). Artificial intelligence, machine learning and deep learning. In 2017 15th International Conference on ICT and Knowledge Engineering (ICT&KE) (pp. 1-6). IEEE.

[14] Litjens, G., Kooi, T., Bejnordi, B. E., Setio, A. A. A., Ciompi, F., Ghafoorian, M., ... & Sánchez, C. I. (2017). A survey on deep learning in medical image analysis. Medical image analysis, 42, 60-88.

[15] Monkam, P., Qi, S., Ma, H., Gao, W., Yao, Y., & Qian, W. (2019). Detection and Classification of Pulmonary Nodules Using Convolutional Neural Networks: A Survey. IEEE Access, 7, 78075–78091. https://doi:10.1109/access.2019.2920980.

[16] Coşkun, M., Yildirim, Ö., Uçar, A., & Demir, Y. (2017). An overview of popular deep learning methods. Eur J Tech, 7(2), 165-176.

[17] LeCun, Y., Bottou, L., Bengio, Y., & Haffner, P. (1998). Gradient-based learning applied to document recognition. Proceedings of the IEEE, 86(11), 2278–2324. https://doi:10.1109/5.726791.

[18] Wang, S., Zhou, M., Liu, Z., Liu, Z., Gu, D., Zang, Y., … Tian, J. (2017). Central focused convolutional neural networks: Developing a data-driven model for lung nodule segmentation. Medical Image Analysis, 40, 172–183. https://doi:10.1016/j.media.2017.06.014.

[19] Krizhevsky, A., Sutskever, I., & Hinton, G. E. (2012). Imagenet classification with deep convolutional neural networks. In: Advances in Neural Information Processing Systems 25.

[20] Szegedy, C., Wei Liu, Yangqing Jia, Sermanet, P., Reed, S., Anguelov, D., … Rabinovich, A. (2015). Going deeper with convolutions. 2015 IEEE Conference on Computer Vision and Pattern Recognition (CVPR). https://doi:10.1109/cvpr.2015.7298594.

[21] He, K., Zhang, X., Ren, S., & Sun, J. (2016). Deep Residual Learning for Image Recognition. 2016 IEEE Conference on Computer Vision and Pattern Recognition (CVPR). https://doi:10.1109/cvpr.2016.90.

[22] Hu, J., Shen, L., Albanie, S., Sun, G., & Wu, E. (2020). Squeeze-and-Excitation Networks. IEEE Transactions on Pattern Analysis and Machine Intelligence, 42(8), 2011–2023. https://doi:10.1109/tpami.2019.2913372.

[23]He, K., Zhang, X., Ren, S., & Sun, J. (2016, October). Identity mappings in deep residual networks. In European conference on computer vision (pp. 630-645). Springer, Cham.

[24]Armato III, S. G., McLennan, G., Bidaut, L., McNitt-Gray, M. F., Meyer, C. R., Reeves, A. P., ... & Kazerooni, E. A. (2011). The lung image database consortium (LIDC) and image database resource initiative (IDRI): a completed reference database of lung nodules on CT scans. Medical physics, 38(2), 915-931.

[25] Jin, H., Li, Z., Tong, R., & Lin, L. (2018). A deep 3D residual CNN for false‐positive reduction in pulmonary nodule detection. Medical physics, 45(5), 2097-2107.

[26] Tajbakhsh, N., & Suzuki, K. (2017). Comparing two classes of end-to-end machine-learning models in lung nodule detection and classification: MTANNs vs. CNNs. Pattern recognition, 63, 476-486.

[27] Sun, W., Zheng, B., & Qian, W. (2017). Automatic feature learning using multichannel ROI based on deep structured algorithms for computerized lung cancer diagnosis. Computers in biology and medicine, 89, 530-539.

[28] de Carvalho Filho, A. O., Silva, A. C., de Paiva, A. C., Nunes, R. A., & Gattass, M. (2017). 3D shape analysis to reduce false positives for lung nodule detection systems. Medical & biological engineering & computing, 55(8), 1199-1213.

[29] Gupta, A., Saar, T., Martens, O., & Moullec, Y. L. (2018). Automatic detection of multisize pulmonary nodules in CT images: Large‐scale validation of the false‐positive reduction step. Medical physics, 45(3), 1135-1149.

[30] Zhang, Y., Sankar, R., & Qian, W. (2007). Boundary delineation in transrectal ultrasound image for prostate cancer. Computers in Biology and Medicine, 37(11), 1591-1599.

[31] Cao, P., Liu, X., Yang, J., Zhao, D., Li, W., Huang, M., & Zaiane, O. (2017). A multi-kernel based framework for heterogeneous feature selection and over-sampling for computer-aided detection of pulmonary nodules. Pattern Recognition, 64, 327-346.

[32] Cao, P., Liu, X., Zhang, J., Li, W., Zhao, D., Huang, M., & Zaiane, O. (2017). A ℓ2, 1 norm regularized multi-kernel learning for false positive reduction in lung nodule

CAD. Computer methods and programs in biomedicine, 140, 211-231.
[33] Parmar, C., Grossmann, P., Bussink, J., Lambin, P., & Aerts, H. J. (2015). Machine learning methods for quantitative radiomic biomarkers. Scientific reports, 5, 13087.
[34] Dhara, A. K., Mukhopadhyay, S., & Khandelwal, N. (2012). Computer-aided detection and analysis of pulmonary nodule from CT images: A survey. IETE Technical Review, 29(4), 265-275.
[35] Meng, Z., Fan, X., Chen, X., Chen, M., & Tong, Y. (2017, August). Detecting small signs from large images. In 2017 IEEE International Conference on Information Reuse and Integration (IRI) (pp. 217-224). IEEE.
[36] Ji, S., Zhang, C., Xu, A., Shi, Y., & Duan, Y. (2018). 3D convolutional neural networks for crop classification with multi-temporal remote sensing images. Remote Sensing, 10(1), 75.
[37] El-Regaily, S. A., Salem, M. A. M., Aziz, M. H. A., & Roushdy, M. I. (2020). Multi-View convolutional neural network for lung nodule false positive reduction. Expert systems with applications, 162, 113017.
[38] Ioffe, S., & Szegedy, C. (2015). Batch normalization: Accelerating deep network training by reducing internal covariate shift. Proceedings of The International Conference on Machine Learning. arXiv preprint arXiv:1502.03167.
[39] He, K., Zhang, X., Ren, S., & Sun, J. (2015). Delving deep into rectifiers: Surpassing human-level performance on imagenet classification. In Proceedings of the IEEE international conference on computer vision (pp. 1026-1034).
[40] Glorot, X., & Bengio, Y. (2010, March). Understanding the difficulty of training deep feedforward neural networks. In Proceedings of the thirteenth international conference on artificial intelligence and statistics (pp. 249-256).
[41] Havaei, M., Davy, A., Warde-Farley, D., Biard, A., Courville, A., Bengio, Y., ... & Larochelle, H. (2017). Brain tumor segmentation with deep neural networks. Medical image analysis, 35, 18-31.
[42] Severyn, A., & Moschitti, A. (2015, June). Unitn: Training deep convolutional neural network for twitter sentiment classification. In Proceedings of the 9th international workshop on semantic evaluation (SemEval 2015) (pp. 464-469).
[43] Golan, R., Jacob, C., & Denzinger, J. (2016, July). Lung nodule detection in CT images using deep convolutional neural networks. In 2016 International Joint Conference on Neural Networks (IJCNN) (pp. 243-250). IEEE.
[44] Bengio, Y. (2012, June). Deep learning of representations for unsupervised and transfer learning. In Proceedings of ICML workshop on unsupervised and transfer learning (pp. 17-36).
[45] Shen, W., Zhou, M., Yang, F., Yang, C., & Tian, J. (2015, June). Multi-scale convolutional neural networks for lung nodule classification. In International Conference on Information Processing in Medical Imaging (pp. 588-599). Springer, Cham.
[46] Shen, W., Zhou, M., Yang, F., Yu, D., Dong, D., Yang, C., ... & Tian, J. (2017). Multi-crop convolutional neural networks for lung nodule malignancy suspiciousness classification. Pattern Recognition, 61, 663-673.
[47] Song, Q., Zhao, L., Luo, X., & Dou, X. (2017). Using deep learning for classification of lung nodules on computed tomography images. Hindawi Journal of Healthcare Engineering. Volume 2017, Article ID 8314740, 7 pages, https://doi.org/10.1155/2017/8314740
[48] Gruetzemacher, R., & Gupta, A. (2016). Using deep learning for pulmonary nodule detection & diagnosis. Twenty-second Americas Conference on Information Systems.
[49] Ypsilantis, P. P., & Montana, G. (2016). Recurrent convolutional networks for pulmonary nodule detection in CT imaging. arXiv preprint arXiv:1609.09143.
[50] Alakwaa, W., Nassef, M., & Badr, A. (2017). Lung cancer detection and classification with 3D convolutional neural network (3D-CNN). (IJACSA) International Journal of Advanced Computer Science and Applications, 8(8), 409.
[51] Wang, B., Qi, G., Tang, S., Zhang, L., Deng, L., & Zhang, Y. (2018, September). Automated pulmonary nodule detection: High sensitivity with few candidates. In International Conference on Medical Image Computing and Computer-Assisted Intervention (pp. 759-767). Springer, Cham.
[52] Xie, H., Yang, D., Sun, N., Chen, Z., & Zhang, Y. (2019). Automated pulmonary nodule detection in CT images using deep convolutional neural networks. Pattern Recognition, 85, 109-119.

[53] Silveira, M., Nascimento, J., & Marques, J. (2007, August). Automatic segmentation of the lungs using robust level sets. In 2007 29th Annual International Conference of the IEEE Engineering in Medicine and Biology Society (pp. 4414-4417). IEEE.

[54] Hassanpour, H., Zehtabian, A., & Yousefian, H. (2011). Pixon-based image segmentation. INTECH Open Access Publisher.